



Supplement of

A comprehensive reappraisal of long-term aerosol characteristics, trends, and variability in Asia

Shikuan Jin et al.

Correspondence to: Yingying Ma (yym863@whu.edu.cn)

The copyright of individual parts of the supplement might differ from the article licence.

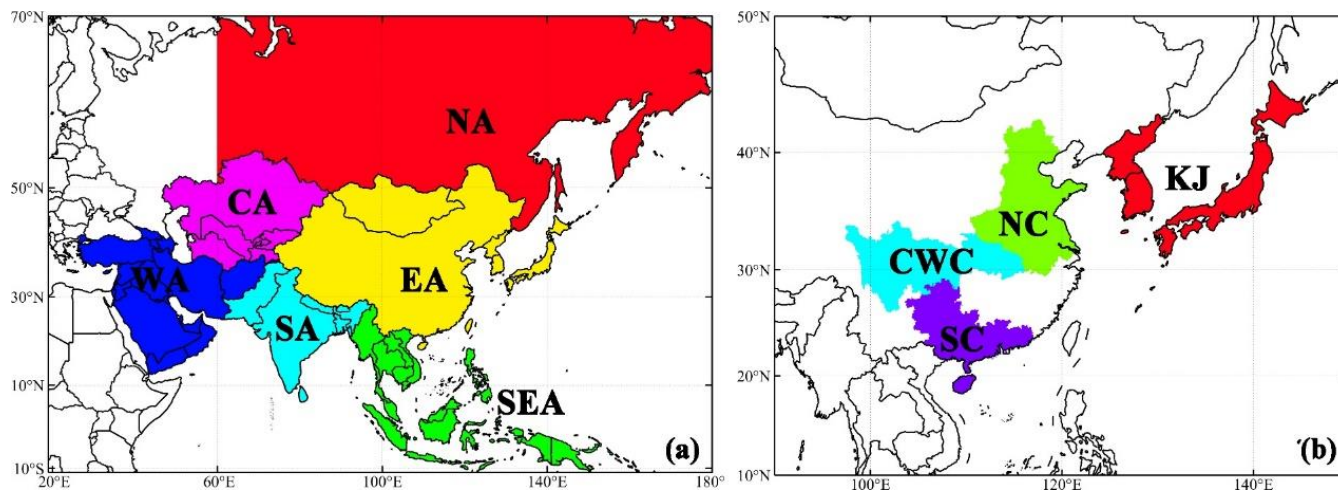
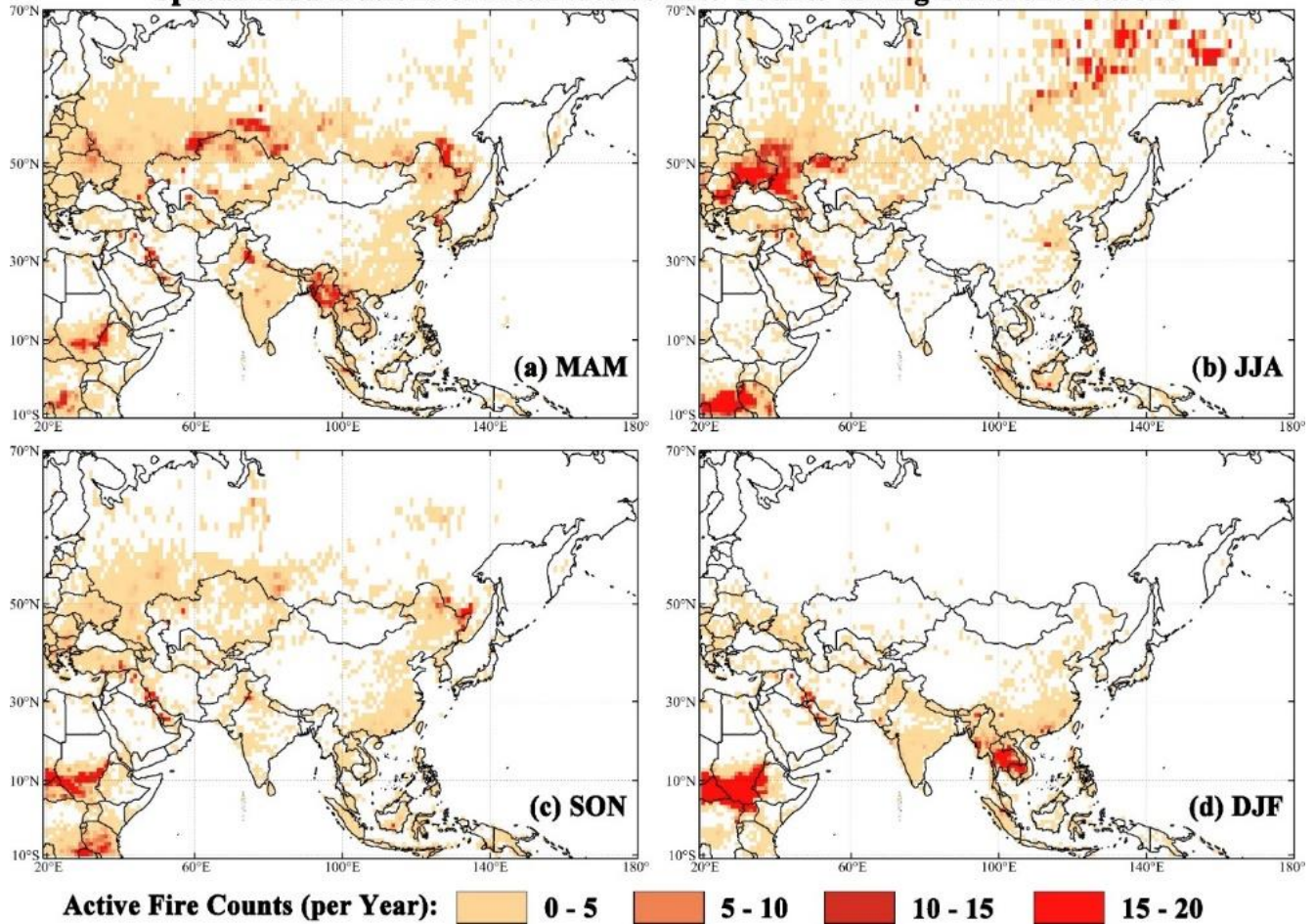


Figure S1. Specific regional divisions of (a) Asia and (b) East Asia (EA) using national or provincial boundaries. For China, our divisions take into account the aerosol research areas that have recently been paid more attention to, 1) the NC refers to the area centered on the North China Plain, including two cities (Beijing and Tianjing) and five provinces (Hebei, Shandong, Henan, Anhui, and Jiangsu); 2) the CWC includes the area (Hubei, Chongqing, and Sichuan) with the main population distribution in central and western China. Especially in Wuhan and Chengdu, these two regions have received a lot of attention in recent years for aerosol changes caused by anthropogenic emissions; 3) the SC is Southern China, including developed provinces of Guangdong, Guangxi, and Hainan. In addition, the major countries centered on the Sea of Japan are also listed separately, denoted as KJ.

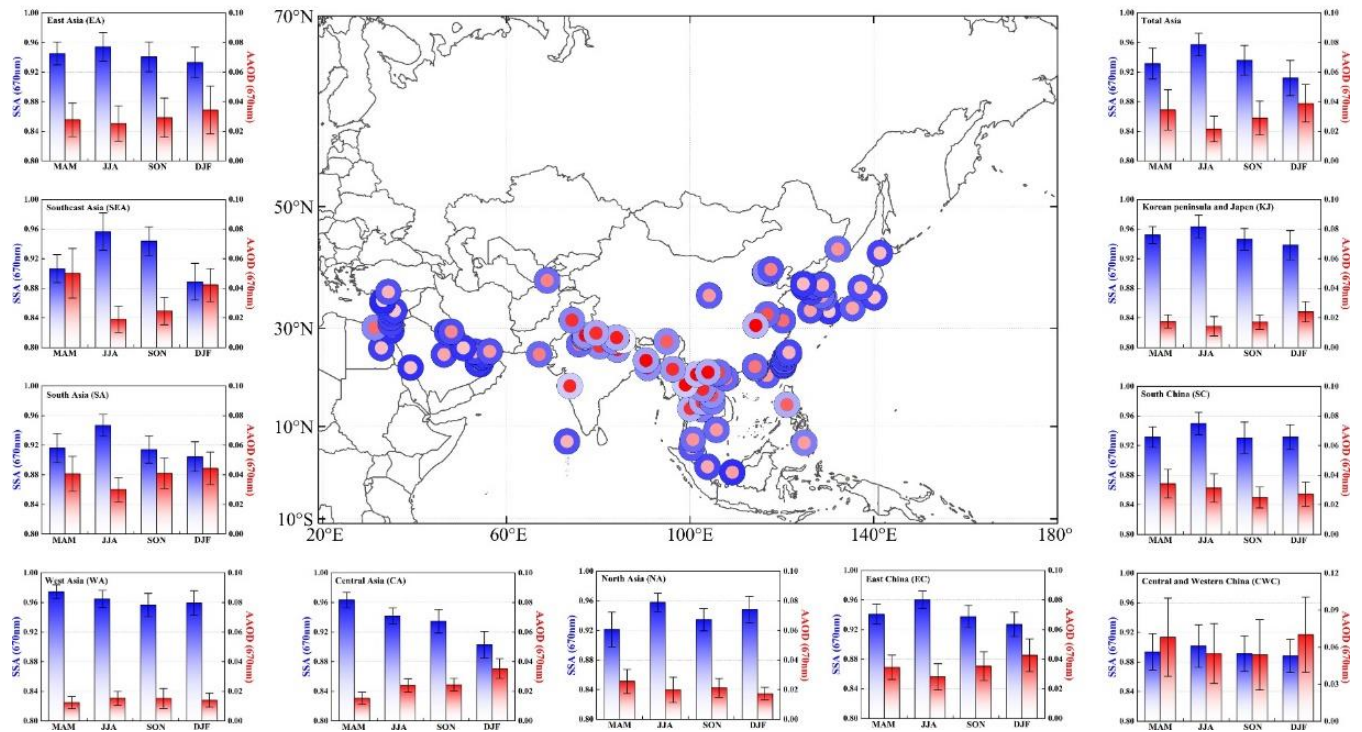
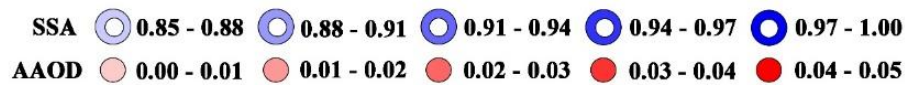
Spatial Distributions of Mean Active Fire Counts during Different Seasons



10

Figure S2. Spatial distributions of annual seasonal active fire counts (confidence $\geq 60\%$) in Asia from 2000 to 2020 from MODIS observations. The deeper the red colour, the more fire points there are. Apart from surrounding regions of WA and CA, the most obvious cluster of fire points occurs in the northern Asia region during summer, which is inferred as wildfires caused by non-human activities.

Spatial Distributions of SSA and AAOD Obtained from AERONET Observations



15

Figure S3. Distributions of absorbing AOD (AAOD) and Single Scattering Albedo (SSA) at 675 nm, obtained from AERONET data in Asia. It must be noting that values from these sites can only partially represent aerosol features in a region, limited by the sparse spatial resolution. Especially, the values of AAOD and SSA in CWC and NA are obtained only from one ground-based sun-photometer in Wuhan and one in Vladivostok, respectively.

20

Table SI. Variance corrected Sen's slope and time of change point in different regions

Region	β' (Total)	Change Year	β' (Before)	β' (After)
Asia	1.38×10^{-4}	2008	2.14×10^{-4}	-1.03×10^{-3} *
EA	-5.28×10^{-4} *	2013 *	5.49×10^{-4}	-1.61×10^{-3} *
SEA	-6.82×10^{-5}	2016	6.59×10^{-4}	-1.59×10^{-4}
SA	1.25×10^{-3} *	2009 *	6.23×10^{-4}	-3.42×10^{-4}
WA	-5.97×10^{-4}	2005	1.33×10^{-3} *	-1.57×10^{-3} *
CA	-1.62×10^{-4}	2015	1.04×10^{-3} *	2.08×10^{-3} *
NA	4.29×10^{-4} *	2008	-7.92×10^{-4}	-8.32×10^{-4}
NC	-1.71×10^{-3} *	2014 *	3.68×10^{-3} *	-6.75×10^{-3} *
CWC	-2.64×10^{-3} *	2012 *	1.97×10^{-3} *	-6.34×10^{-3} *
SC	-5.24×10^{-3} *	2014 *	3.15×10^{-3}	-7.55×10^{-3} *
KJ	-8.00×10^{-4} *	2012 *	8.55×10^{-4}	-3.26×10^{-3} *

Note: Change year represents the time at which the abruption occurred. β' (Before) and β' (After) are trends from 2000 to change year and from change year to 2020, respectively. Significant test * $p < 0.05$.